Hindawi
Advances in Polymer Technology
Volume 2019, Article ID 4523696, 11 pages
https://doi.org/10.1155/2019/4523696

Research Article

Mechanical Properties and Mullins Effect in Natural Rubber Reinforced by Grafted Carbon Black

Wen Fu,[1] **Li Wang**,[2] **Jianning Huang**,[1] **Cuiwen Liu**,[1] **Wenlong Peng**,[1] **Haotuo Xiao**,[1] **and Shenglin Li**[1]

[1]*College of Material Science, Guangdong University of Petrochemical Technology, Maoming, Guangdong 525000, China*
[2]*College of Chemical Engineering, Guangdong University of Petrochemical Technology, Maoming, Guangdong 525000, China*

Correspondence should be addressed to Li Wang; wanglihaha@126.com

Received 18 June 2019; Accepted 11 July 2019; Published 1 August 2019

Guest Editor: Zhiwei Qiao

The obvious polarity difference between the carbon black (CB) and the natural rubber (NR) causes the CB hard to be dispersed in the NR matrix when the addition amount is large. In this paper, polyethylene glycol (PEG) was grafted onto the surface of CB by the liquid phase. The grafted carbon black (GCB) was prepared and applied to reinforce NR. The main physical and mechanical properties of NR were improved because of the better compatibility between GCB and NR. The Mullins effect of the vulcanizate was calculated by the cyclic stress-strain experiment. The results showed that the Mullins effect both existed in the virgin NR system and filled NR system. The degree of Mullins effect was increased with the increase of the filler addition, but that was different for CB and GCB. When the filler addition was below 20 phr, the Mullins effect of NR/GCB was stronger than that of NR/CB. However, when the filler addition was over 30 phr, the Mullins effect of NR/CB was stronger than that of NR/GCB. The Mullins effect was affected by the heat treatment temperature and time. The mechanisms of the Mullins effect were analyzed.

1. Introduction

Because the rubber materials have high elasticity, damping, and other excellent properties, they have been widely used in tires, electronics, military, aerospace, and other fields [1–3]. In general, the physical and mechanical properties of the pure rubber are not very good, so the rubber materials need to be reinforced in order to improve their comprehensive performance. Carbon black is the main reinforcement agent in the rubber industry [2–4]. Since CB is a polar material and NR is a nonpolar material, the polarity difference between CB and NR is obvious, so the dispersion of CB in the NR matrix is difficult when the amount of CB is large, thereby causing the decrease of the physical and mechanical properties of NR. Grafting some polymer chains on the surface of CB to reduce the polarity difference between CB and the matrix is a good strategy, thereby enhancing the reinforcing effect of CB.

Chen [5] used the radiation grafting method to graft the polyethylene (PE) on the surface of carbon black. The grafting ratio of PE onto the carbon black surface proceeded and the percentage of grafting exceeded 90% when the irradiation dose reached 200 kGy. Tsubokawa [6] investigated the surface grafting of hyperbranched poly(amidoamine) onto the surface by using dendrimer synthesis methodology. The percentage of poly(amidoamine) grafting reached 96.2% after 10th generation. Richner [7] grafted the isocyanate prepolymers on the surface of CB. This crosslinked carbon black was designed as a new active material for electrochemical electrodes, and the active material for electric double-layer capacitor electrodes was produced which had a specific capacitance of up to 200 F/g. Yang [8] first synthesized the polystyrene, poly(styrene-co-maleic anhydride), poly[styrene-co-(4-vinylpyridine)], and poly(4-vinylpyridine). Then, the resultant polymers were grafted onto the surface of carbon black through a radical trapping reaction. It was found that the carbon black grafted with polystyrene and poly(styrene-co-maleic anhydride) could be dispersed in tetrahydrofuran, chloroform, dichloromethane, N, N-dimethylformamide, etc., and the carbon black

grafted with poly(4-vinylpyridine) and poly[styrene-co-(4-vinylpyridine)] could be well dispersed in ethanol.

The required stress at the same certain strain was decreased after cyclic tension treatment for several times in the vulcanized rubber composites, which was called the strain softening effect or Mullins effect [9]. This effect was discovered by Bouasse and Carriere [10]. More following works by Mullins pointed out that the Mullins effect not only existed in the filled rubber system, but also in the unfilled rubber system. However, the Mullins effect of the unfilled rubber system was weaker than that of the filled rubber system [11, 12]. Other similar researches about the Mullins effect had been conducted, for example, the rubber matrix (nitrile rubber [13], ethylene propylene diene rubber [14], natural rubber [15], and styrene butadiene rubber [16]) with carbon black [17], silica [18], and other fillers [19].

Some explanatory models were proposed to explain the Mullins effect. Bueche [20] pointed out that it was a proportional relationship between the space change of microparticles and the macroscopic deformation. With the increase of the macroscopic deformation, the rubber molecular chains among filler particles achieved their ultimate elongation, and some molecular chains would be broken away from the filler surfaces, leading to a decrease of the interaction force between the molecular chains and fillers, finally causing the Mullins effect. Houwink [21] put forward that the Mullins effect resulted from the slipping of the molecular chains adsorbed on the filler surface during the stretching process. Mullins [11] insisted that the filled vulcanized rubber was a hybrid system consisted of the high filler content region (hard phase) and low filler content region (soft phase). During the deformation process, the hard phase would be transferred to the soft phase, which led to the Mullins effect. This view was further perfected by Johnson [22]. He pointed out that the short molecular chains in the vulcanized rubber system would be tangled to form the molecular chain clusters, followed by the formation of hard phase in the internal. Some molecular chains of the hard phase were pulled out and transferred into the soft phase during the deformation process. Kraus [23] thought that the Mullins effect was the combination of several effects, including the destruction of the filler aggregate network and the destruction of the filler-rubber molecular interaction. Hamed [24] noted that the rubber molecular chains could adsorb on the filler surface to form a rubber shell layer. Under the external force, the rubber molecular chains adsorbed on the surface of fillers would be desorbed, thus reducing the thickness of the rubber shell and weakening the interaction between the rubber and carbon black. Roozbeh [12] mentioned that the filled rubber system contained two kinds of cross-linking networks, the molecular chains cross-linking network of the rubber matrix, and the interaction network of the filler-filler and filler-matrix. The Mullins effect was the result of the interaction between these two kinds of cross-linking networks. Until now, these models are still controversial, none of which can provide a reasonable and complete explanation for the Mullins effect. Table 1 showed the related diagrams of mechanism models of the Mullins effect.

In this work, in order to reduce the polarity difference between CB and NR and improve the dispersion of CB in the NR matrix, CB was graft modified with PEG and applied to reinforce NR. The comprehensive performance of NR has been increased with the addition of GCB. More importantly, the Mullins effect mechanisms were deduced by comparing the effects of GCB and CB on the Mullins effect of NR under different conditions.

2. Experiments

2.1. Materials. Natural rubber (NR, type of 3L) was purchased from Guangzhou Beishite Company, China. Carbon black (CB, type of N330, the average diameter size of 25~30 nm, the specific surface area of 103 m^2/g) was obtained from Cabot Corporation, USA. Concentrated nitric acid, toluene, thionyl chloride, dibutyl dilaurate, zinc oxide (ZnO), stearic acid (SA), and polyethylene glycol (PEG, number-average molecular weight of 400) were analytically pure and purchased from Sigma Aldrich Company, USA. Poly(1,2-dihydro-2,2,4-trimethyl-quinoline (antioxidant RD), 2,2′-dibenzothiazole disulfide (accelerator DM) and sulfur (S) were purchased directly from the market and used as received.

2.2. Sample Preparation

2.2.1. The Preparation of Grafted Carbon Black. 50 g of CB and 350 ml of concentrated nitric acid were added to a 1000 ml three-neck flask, the samples were reacted at 60°C for 2 h using the mechanical stirring, and then the reaction product was filtered, washed with deionized water, dried at 95°C to obtain the intermediate A. 50 g of the intermediate A, 12.5 g of thionyl chloride, and 350 ml of toluene were placed in a 1000 ml three-neck flask, and the samples were reacted at 0°C for 30 min and then at 120°C for 30 min using the mechanical stirring. The reaction product was rotary evaporated at 80°C to remove the unreacted thionyl chloride; the intermediate B was prepared. Subsequently, 50 g of the intermediate B, 25 g of PEG, 0.1 ml of dibutyl dilaurate, and 350 ml of toluene were added to a 1000 ml three-neck flask; the samples were reacted 0°C for 30 min and then at 120°C for 1 h using the mechanical stirring. The reaction product was filtered, washed with deionized water, dried at 95°C to obtain the grafted carbon black, denoted as GCB.

2.2.2. The Preparation of NR/CB and NR/GCB Vulcanizates. The roller gap of two-roll mill was adjusted to about 2 mm, NR was added and plasticated for 8 minutes, and then CB (or GCB), ZnO, SA, RD, DM, and S were added to the two-roll mill in turn, followed by 5 times side cuts on the left and right, and then a triangle package was implemented 7 times and thin-passing for 8 times. Subsequently, the compounds were stored for 24 h and were cured by a press vulcanizer at 150°C for (t_{90}+2) min. The mass ratio of NR, ZnO, SA, RD, DM, and S was 100: 5: 2: 1: 1: 2. The filler contents were varied from 0 to 60 phr.

Table 1: Schematic diagrams of Mullins effect mechanisms.

Models	Schematic diagrams
Detachment of the molecular chains [20]	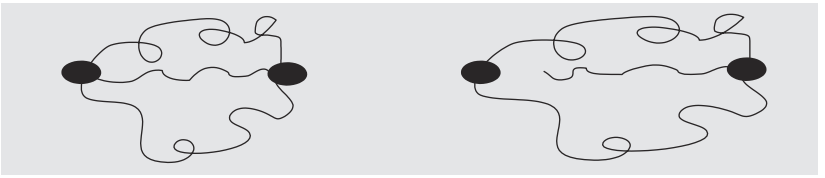
Slippage of the molecular chains [21]	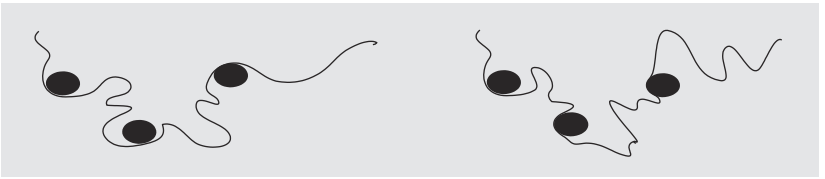
Disentanglement of the rubber molecular chains [11, 22]	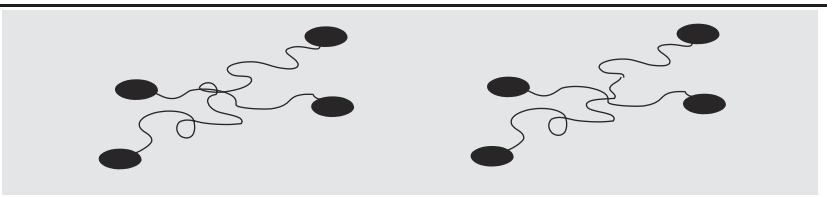
Destruction of the filler aggregates [23]	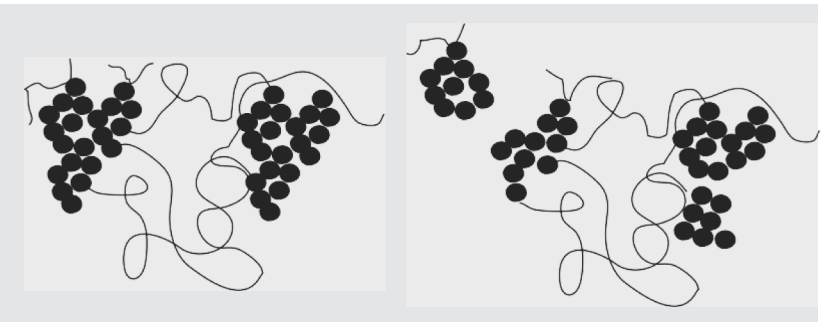
Rubber shell model [24]	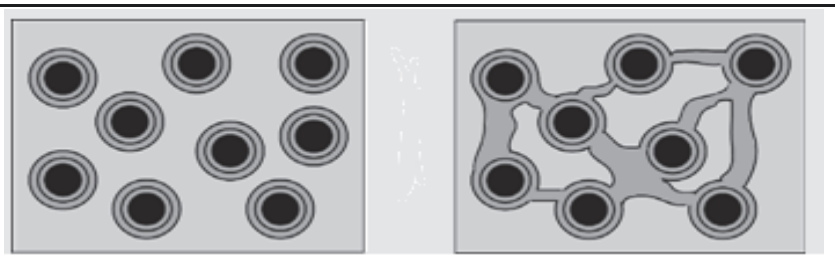

2.3. Characterization

2.3.1. Thermogravimetric Analysis. The thermogravimetric analyzer (TGA, 209 F3, Netzsch, Germany) was used to test the graft ratio of PEG on CB. The temperature range was 30~850°C, the heating rate was 50 K/min, and the test atmosphere was nitrogen. In order to remove the PEG adsorbed on the surface of CB through physical adsorption, GCB was purified by reflux condensation for 0.5 h with toluene and then dried.

2.3.2. Physical and Mechanical Properties Test. The electronic tensile testing machine (GT-TCS-2000, Gaotie, China) was used to test the tensile and tear properties. The tensile strength was characterized according to GB/T 528-2009, the tensile speed was 200 mm/min, the thickness was 2.0 mm, and the sample shape was dumbbell-shaped. The tear strength was tested according to GB/T 529-2008; the sample shape was right angle. The Shore A hardness was determined according to GB/T 531-1999. The wear resistance was measured according to GB/T 9867-2008. The apparent crosslink density was tested by the swelling method. About 1 g of the vulcanizate was weighed and cut into small strips about 2 mm wide and 1 mm thick and the treated samples were stored in a container with toluene for 7 d at room temperature. After completing the swelling process, these strips were taken out, and then the toluene adsorbed on the surface of these strips was removed using the filter paper; subsequently, these strips were weighed. The crosslink density was calculated according to the Nory-Rehner formula [25] as follows:

$$\nu_r = \frac{1}{v}\left[\frac{\ln\left(1-\nu_2\right)+\nu_2+\chi{\nu_2}^2}{{\nu_2}^{1/3}-\nu_2/2}\right] \quad (1)$$

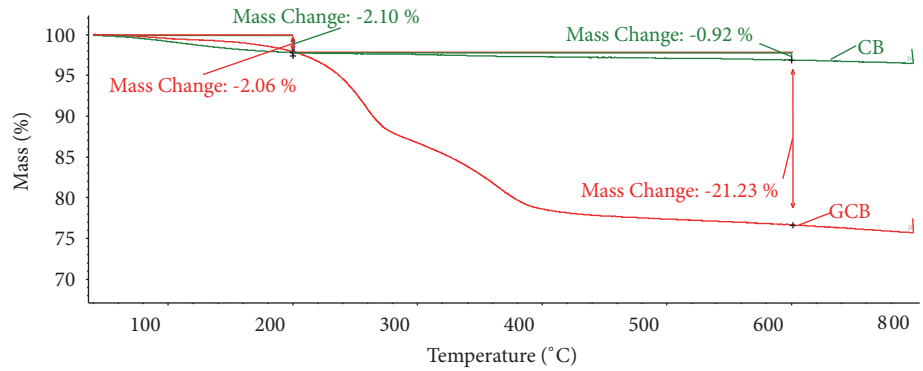

Figure 1: TGA analysis of carbon black before and after modification.

v_r is the apparent crosslink density of the vulcanizate, v_2 is the volume fraction of the rubber phase in the vulcanizate, χ is the interaction parameters between the rubber and solvent, v is the molar volume of the solvent.

where v_2 was calculated according to the formula

$$v_2 = \frac{m_3/\rho}{m_3/\rho + (m_2 - m_1)/\rho_s} \quad (2)$$

ρ_s is the density of the solvent, ρ is the density of the rubber phase, m_1 is the quality of the vulcanizate before swelling, m_2 is the quality of the vulcanizate after swelling, m_3 is the quality of the rubber phase.

2.3.3. Mullins Effect Test. The Mullins effect of the vulcanizate was calculated by the cyclic stress-strain experiment [26]. The sample was stretched to the specified strain for the first time and the required energy was recorded as W_1; the same sample was stretched to the same strain for the second time and the required energy was recorded as W_2. Generally speaking, the value of W_2 was less than that of W_1, the phenomenon was called the strain softening or Mullins effect, and the value of W_2/W_1 was used to represent the degree of the Mullins effect. In this work, the same sample was stretched to the specified strain at room temperature for the first, second, third, and fourth times and the required energies were recorded as W_1, W_2, W_3, and W_4, respectively. According to some repetitive experiments, it was found that the value of W_4 was similar to that of W_3. Hence, after the sample was stretched three times, the Mullins effect was stabilized. In order to test the effect of the treatment temperature and storage time on the Mullins effect, after the sample was stretched three times, the sample was stored for 2 h at 60°C, and then the sample was stretched to the same specified strain at room temperature and the required energy was recorded as W_s. The Mullins effects in different cases were calculated using the following formulas:

$$M_1 = \frac{[(W_1(\varepsilon) - W_3(\varepsilon)]}{W_1(\varepsilon)} * 100\% \quad (3)$$

$$M_2 = \frac{[(W_1(\varepsilon) - W_s(\varepsilon)]}{W_1(\varepsilon)} * 100\% \quad (4)$$

M_1 is the degree of the Mullins effect after stretching for three times at room temperature and M_2 is the degree of the Mullins effect after recovery at 60°C for 2 h.

3. Results and Discussion

3.1. The Graft Ratio of PEG on CB. Due to the large difference in polarity between CB and NR, it is difficult for CB to be uniformly dispersed in the rubber matrix, especially when the amount of CB is large, thereby affecting the physical and mechanical properties of the rubber. The difference in polarity between CB and NR can be reduced by the graft modification of CB. Hence, the dispersibility of CB in the rubber matrix is improved significantly, so the physical and mechanical properties of the rubber are improved. The graft ratio of PEG on CB was measured through the TGA curves of CB and GCB (Figure 1). It can be seen from the figure that the mass loss of CB from 30°C to 200°C was 2.1%. It was due to the loss of the water adsorbed on the surface of CB. The mass loss of CB from 200°C to 650°C was 0.92%. It was attributed to the carbonization of the organic components in CB. While for the GCB sample, the mass loss from 200°C to 650°C was 21.23%, which was obviously higher than that of CB. The reason was the PEG was grafted on the surface of CB and it was burned down during the high temperature process, so the graft ratio of PEG on CB could be measured according the TGA curve; the value was about 20%.

3.2. Physical and Mechanical Properties of NR/CB and NR/GCB. Figures 2(a)–2(f) were the physical and mechanical properties of the NR/CB and NR/GCB composites at different filler contents. It can be seen from Figures 2(a)–2(e) that with the increase of the addition amount of CB, the tear strength and shore A hardness were increased gradually, the elongation at break was decreased gradually, and the modulus at 300% and tensile strength of the vulcanizate were first increased and then decreased. When the CB content was 50 phr, the modulus at 300% and tensile strength reached the highest; the values were 6.3 Mpa and 21.2 Mpa, respectively. However, when the CB content was increased to 60 phr, the modulus at 300% and tensile strength were decreased. Since CB was hard to be dispersed in the rubber matrix when the addition amount was large, hence the filler 3D network

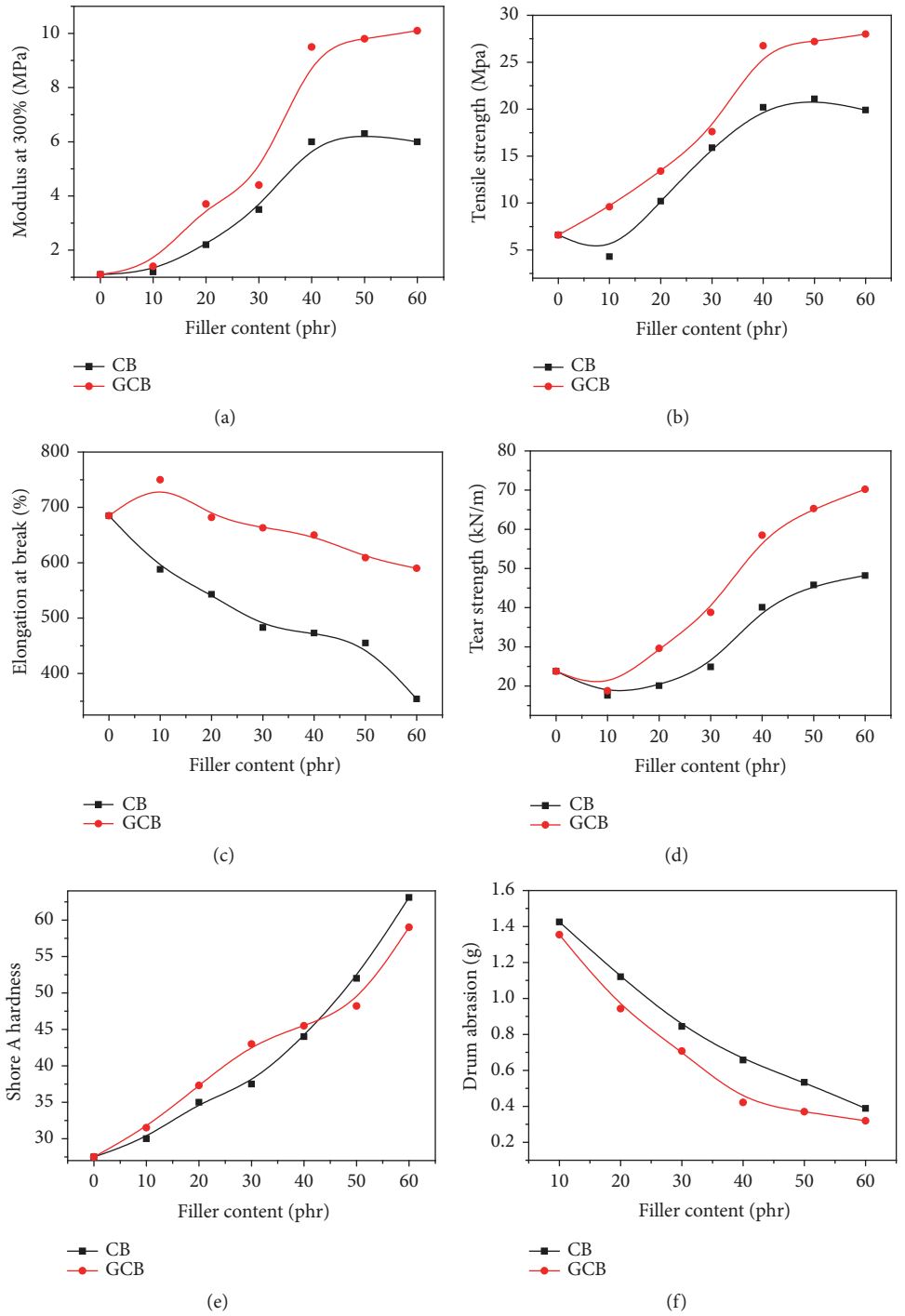

Figure 2: Physical and mechanical properties of NR/CB and NR/GCB.

structure was formed and the aggregation of fillers occurred; the mechanical properties were affected [27].

For the NR/GCB composites, with the increase of the addition amount of GCB, the modulus at 300%, tensile strength, tear strength, and shore A hardness were increased gradually. Unlike the NR/CB composites, the optimum values of the modulus at 300%, tensile strength, tear strength, and shore A hardness were shown when the addition amount of GCB was 60 phr. In addition, the modulus at 300%, tensile strength, elongation at break, and tear strength of NR/GCB were always bigger than that of NR/CB at the same filler content. Compared with the NR/CB composites, the increase rates of the modulus at 300%, tensile strength, elongation at break, and tear strength of NR/GCB were 55.6%, 28.3%, 33.8%, and 42.6%, respectively, when the filler content was 50 phr. It indicated that the addition of GCB could greatly improve the comprehensive physical and mechanical properties of the rubber. Since GCB can be better dispersed in the

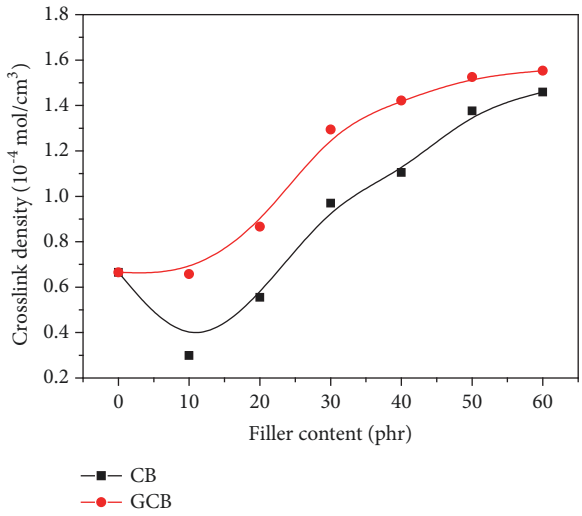

Figure 3: Apparent crosslink densities of NR/CB and NR/GCB.

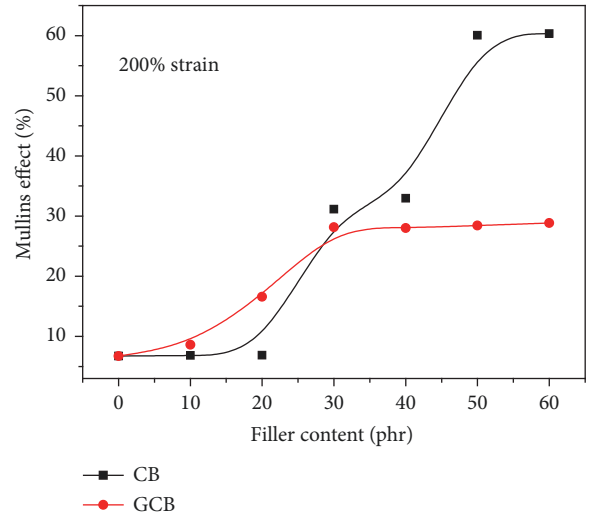

Figure 4: Effect of filler content on Mullins effect of NR/CB and NR/GCB.

rubber matrix, it is less likely to form filler aggregation, and the interaction between GCB and NR was stronger; thereby the physical and mechanical properties were improved.

The wear resistances of NR/CB and NR/GCB with the different filler content were shown in Figure 2(f). With the increase of filler content, the mass of absolute abrasion was decreased gradually, which indicated that the addition of CB or GCB was helpful for improving the wear resistance of NR. The wear resistance of NR/GCB was better than that of NR/CB when the filler content was the same. It is mainly because the NR/GCB has better dispersibility of the filler, larger filler-rubber interaction, and better tear resistance, which is beneficial to hinder the generation of cracks and branch cracks and thus improve the wear resistance [28].

3.3. Apparent Crosslink Densities of NR/CB and NR/GCB. The apparent crosslink density is a representation of the degree of vulcanization, including the chemical crosslinks (polysulfidic, disulfidic, and monosulfidic), as well as the physical crosslinks (rubber-filler interaction and filler-filler network) [29]. The apparent crosslink densities of the NR/CB and NR/GCB vulcanizates at different filler additions were shown in Figure 3. It can be seen from the figure that the apparent crosslink density of the virgin NR vulcanizate was 0.67×10^{-4} mol/cm^3. When the amount of the filler was 10 phr, the apparent crosslink densities of the NR/CB and NR/GCB vulcanizates were decreased to 0.30×10^{-4} mol/cm^3 and 0.66×10^{-4} mol/cm^3, respectively. This is because the N330 carbon black is alkaline, but the accelerator DM is acidic. When CB is added to the rubber system, DM is adsorbed by CB, resulting in a decrease of DM involved in the crosslinking reaction, thereby causing a decrease of the crosslink density. Thereafter, the apparent crosslink densities of the NR/CB and NR/GCB vulcanizates were increased gradually as the amount of filler increased. It is due to more and more rubber-filler interaction and filler-filler network generation with the increase of the filler content [29]. In addition, the apparent crosslink density of NR/GCB was bigger than that of NR/CB at the same amount of filler. This is because GCB has better dispersion in the rubber matrix and thus more filler-rubber interaction was created.

3.4. Effect of Filler Content on Mullins Effect of NR/CB and NR/GCB. The effect of filler content on Mullins effect of NR/CB and NR/GCB composites was shown in Figure 4. It can be seen from the figure that when the sample was stretched after three times at room temperature to make the Mullins effect stability, the degree of Mullins effect of the virgin NR was 6.12%. It is mainly due to the physical disentanglement of rubber molecular chains during the stretching process [11].

In addition, the degree of Mullins effect was increased as the increase of filler addition amount whatever CB or GCB was added to the rubber matrix, but the increase rate in the Mullins effect of adding CB or GCB was different. When the filler addition was below 20 phr, the Mullins effect of NR/GCB was stronger than that of NR/CB. This is because when the amount of filler is smaller than 20 phr, the filler particles are only dispersed in the rubber matrix in isolation and they are unlikely to form a filler-filler 3D network structure [12]. The Mullins effect at this time should be resulted from the disentanglement of rubber molecular chains and destruction of the filler-rubber interaction during the stretching process. In the case of the same amount of rubber matrix, the Mullins effect caused by the disentanglement of rubber molecular chains is similar, so the Mullins effect should be mainly caused by the destruction of the filler-rubber interaction [20]. The destruction is mainly achieved by the rubber molecular chains' shedding and slippage from the surface of fillers. That is, the mechanism of the Mullins effect at low filler content is due to the molecular chains' shedding and slippage mechanism. The dispersion of GCB in the rubber matrix is improved compared to CB, and the compatibility with the rubber matrix is also increased. Hence, more filler-rubber interactions are formed on the microscopic level. These

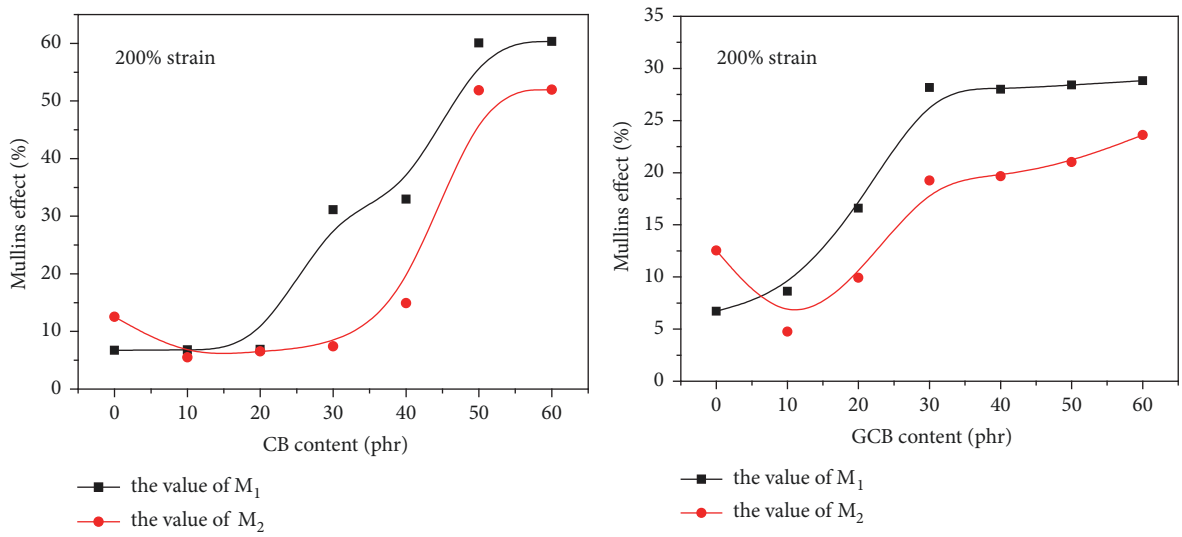

Figure 5: Effect of storage on Mullins effect of NR/CB and NR/GCB.

interactions are destroyed during the stretching process, thus resulting in greater Mullins effect.

However, when the filler addition was over 30 phr, the Mullins effect of NR/CB was stronger than that of NR/GCB. Particularly, when the filler addition was 60 phr, the degree of Mullins effect of NR/GCB was only 47% of that of NR/CB. This is because when the amount of CB is over 30 phr, the filler-filler 3D network structures as a new factor affecting the Mullins effect began to appear, and when the amount of CB reached to 60 phr, these filler-filler 3D network structures were already intense. The filler-filler 3D network structure can be destroyed during the stretching process, thus leading to obvious Mullins effect [23]. Nevertheless, for NR/GCB, fewer filler-filler 3D network structures were generated because GCB has better dispersion in the rubber matrix, so the Mullins effect of NR/GCB was not serious even if the amount of filler was large.

Moreover, when the amount of CB was increased from 40 phr to 50 phr, the Mullins effect rose sharply from 33% to 60%. Some authors called this phenomenon a percolation transition of filler reinforcement [30]. At this time, various isolated filler-filler 3D network structures are connected to each other as a whole. This whole is destroyed during the stretching process, which leads to a sharp rise in the Mullins effect. However, this sudden increase of the Mullins effect did not occur in NR/GCB when the amount of filler was increased from 40 phr to 50 phr, nor did it occur when the amount of filler was increased from 50 phr to 60 phr. It was also shown that CB can be dispersed more uniformly after the graft modification, and it is more difficult to form the filler-filler 3D network structure in the rubber matrix.

3.5. Effect of Storage on Mullins Effect Recovery of NR/CB and NR/GCB. Studying the changes in the Mullins effect during the storage is helpful for further understanding the mechanism of the Mullins effect. According to formula (3) and formula (4), the values of M_1 and M_2 of the NR/CB and NR/GCB samples were calculated and shown in Figures 5(a) and 5(b). It can be seen from the figure that when no filler was added, the value of M_2 of the virgin NR vulcanizate was bigger than that of M_1. According to the previous analysis, the factor that causes the Mullins effect at this time is only the physical disentanglement of rubber molecular chains during the stretching process. So it means that the high temperature treatment is good for re-entanglement of the rubber molecular chains [31]. This is because the activity of the rubber molecular chains rises; thus more re-entanglements are generated during the high temperature treatment process. More re-entanglements are destroyed during the stretching process and lead to bigger Mullins effect.

In addition, when the filler content is from 10 phr to 60 phr, with the increase of the filler content, the Mullins effect was increased gradually during the high temperature treatment process. But the values of M_2 of the NR/CB and NR/GCB samples were smaller than the values of M_1 of their counterparts. It indicates that the high temperature treatment is beneficial for the regeneration of the filler-rubber interaction and filler-filler 3D network structure [31]. However, it is only partial regeneration, and it is hard to return to the initial state of the filler-rubber interaction and filler-filler 3D network structure, so the value of M_2 is always smaller than the value of M_1 at the same filler addition.

3.6. Effect of Storage on Mullins Effect Recovery of NR/CB and NR/GCB. The phenomenological theory is a research method of rubber elasticity theory. The Mooney-Rivlin equation is one of the most commonly used expressions in the phenomenological theory [32], which is shown as follows:

$$\frac{\sigma}{\lambda - \lambda^{-2}} = 2C_{10} + 2C_{01}\left(\frac{1}{\lambda}\right) \quad (5)$$

In formula (5), σ is the stress, $\sigma/(\lambda - \lambda^{-2})$ is defined as the reduced stress, λ is the strain along the stress direction, and C_{10} and C_{01} are constants without clear physical meaning [33].

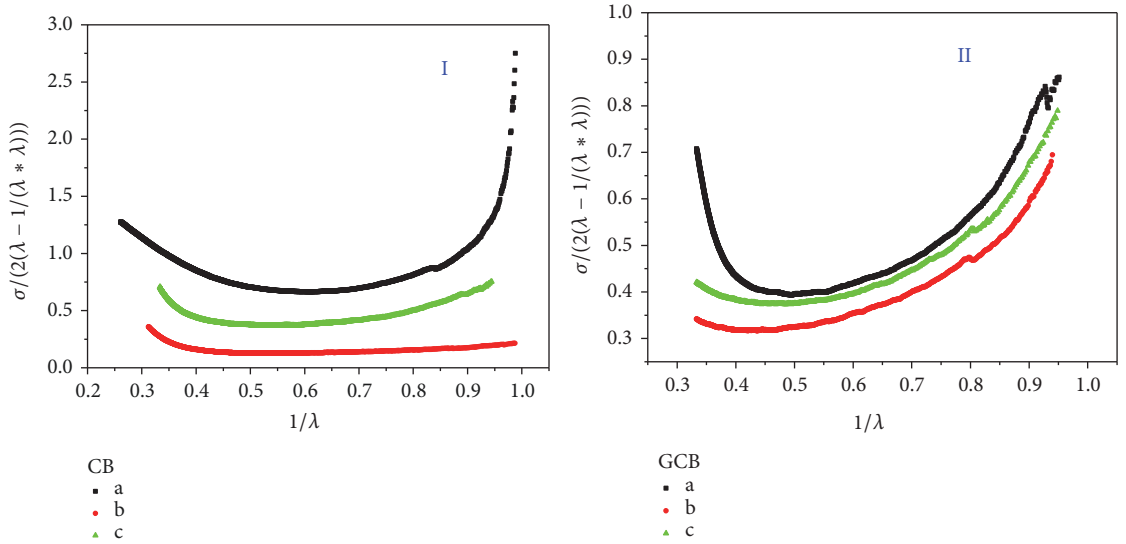

Figure 6: Mooney curves of NR/CB and NR/GCB at different conditions.

According to the formula (5), the stress-strain curve of a sample can be transferred to the Mooney-Rivlin curve (hereinafter referred to as Mooney curve). The Mooney curves of the sample being directly stretched to break, the sample being repeatedly stretched to 200% strain for 3 times and then stretched to break, and the sample being repeatedly stretched to 200% strain for 3 times and then placed in an oven at 60°C for 2 h and then stretched to break were shown in Figure 6. The CB or GCB filler content was 60 phr in this experiment. According to the formula (5), the ideal Mooney curve should be a straight line. But it can be seen from the Figure 6 that the real Mooney curve was not a straight line. The reduced stress $\sigma/(\lambda - \lambda^{-2})$ first fell and then rose with the increase of the strain λ (look from the right to left of the curves), presented a "U-shaped" trend. The difference of the ideal Mooney curve and real Mooney curve reflects two additive effects during the stretching process: (1) in the low strain region (the right side of the curve), the reduced stress decrease with the increase of strain is due to the Mullins effect of the material. (2) In the high strain region (the left side of the curve), the reduced stress increases with the increase of strain is because of the non-Gaussian behavior of the polymer chains. The upturning phenomenon of the reduced stress in high strain region indicates that the polymer chains are stretched to their ultimate elongation [33].

The Mooney curve of the NR/CB sample being directly stretched to break (Figure 6(I-a)) showed a very obvious decline in the low strain region. It indicated an obvious Mullins effect occurred. However, when the sample was repeatedly stretched to 200% strain for 3 times and then stretched to break, the Mooney curve in the low strain region (Figure 6(I-b)) did not show a significant decline. This is because the repeated stretching leads to the disentanglement of rubber molecular chains, the destruction of the filler-rubber interaction, and filler-filler 3D network structure, thus leading to the decrease of the Mullins effect. The destruction of the filler-filler 3D network structure should be the main cause of the decline of the Mullins effect. When the sample was treated in an oven at 60°C for 2 h after it has been stretched for 3 times, the Mooney curve in the low strain region (Figure 6(I-c)) presented a relatively significant decline compared to Figure 6(I-b). The reason is that the rubber molecular chains are re-entangled; the filler-rubber interaction and filler-filler 3D network structure are regenerated during the high temperature treatment process. In addition, Figure 6(I-b) curve was always below Figure 6(I-a) curve and Figure 6(I-c) curve was always above Figure 6(I-b) curve. It meant that the stress required for Figure 6(I-b) curve was smaller than that of Figure 6(I-a) curve and the stress required for Figure 6(I-c) curve was bigger than that of Figure 6(I-b) curve at the same strain. It also indicates that the repeated stretching leads to the disentanglement of rubber molecular chains, the destruction of the filler-rubber interaction and filler-filler 3D network structure; the high temperature treatment is helpful for the re-entanglement of rubber molecular chains and the regeneration of the filler-rubber interaction and filler-filler 3D network structure.

The trend of the Mooney curves of the NR/GCB samples under the three different stretching conditions (Figure 6(I-a, b, c)) was similar to that of the NR/CB samples (Figure 6(II-a, b, c)), but there were some differences that had to be mentioned. First, when λ^{-1} was changed from 1.0 to 0.9, the value of $\sigma/2(\lambda - \lambda^{-2})$ of NR/CB was changed from 2.72 to 0.98. However, the value of $\sigma/2(\lambda - \lambda^{-2})$ of NR/GCB was changed from 0.86 to 0.76, which was obviously smaller than that of NR/CB. This also showed that the Mullins effect of NR/GCB was lower when the filler content was 60 phr. Second, whatever being directly stretched to break (Figure 6(II-a)), being repeatedly stretched to 200% strain for 3 times and then stretched to break (Figure 6(II-b)), and being repeatedly stretched to 200% strain for 3 times and then placed in an oven at 60°C for 2 h and then stretched to break (Figure 6(II-c)), the Mooney curves of the samples in the low strain region all presented a relatively significant decline. It

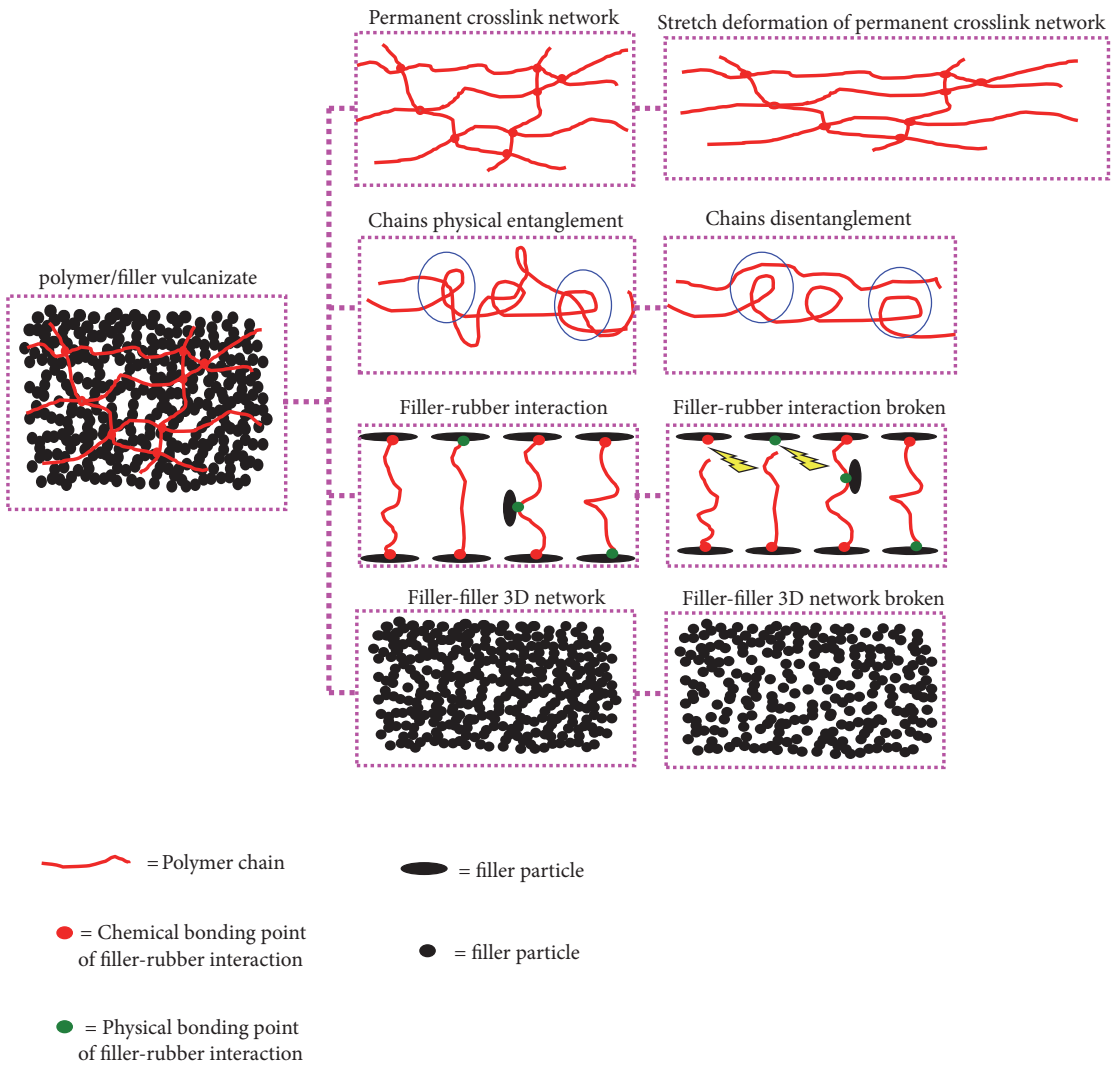

Figure 7: Filler reinforcement and Mullins effect mechanisms.

illustrates that the reason causing the Mullins effect of NR/CB and the Mullins effect of NR/GCB is different. The main reason causing the Mullins effect of NR/CB is the destruction of the filler-filler 3D network structure, while the main reason causing the Mullins effect of NR/GCB is the destruction of the filler-rubber interaction.

3.7. Filler Reinforcement and Mullins Effect Mechanisms. Combining the previous analyses and drawing on Roozbeh's viewpoint [12], the polymer/filler vulcanizate system can be divided into four parts: the permanent crosslink network of polymer chains crosslinked by the vulcanizing agents (Figure 7, row 1), the physical entanglement network of polymer chains (Figure 7, row 2), the filler-rubber interaction system (Figure 7, row 3), and the filler-filler 3D network system (Figure 7, row 4). The combined action of these four parts constitutes the reinforcing mechanisms of polymer/filler vulcanizate system, and the Mullins effect mechanisms are also caused by the changes of these four parts at different situations. The filler reinforcement and Mullins effect mechanisms are analyzed as follows:

(1) For the virgin polymer vulcanizate system with no filler, the strength of the vulcanizate is derived from the orientation and fracture of the polymer permanent crosslink network and the crystallization owing to the orientation of the polymer chains during the stretching process [34]. While the Mullins effect should be mainly attributed to the disentanglement of the polymer chains during the stretching process (Figure 7, row 2), and the Mullins effect caused by this disentanglement is weak.

(2) For the polymer vulcanizate system with low filler content, the orientation and fracture of the polymer permanent crosslink network and the crystallization can result in the strength improvement; the filler-rubber interaction is another factor to lead to the strength improvement of the vulcanizate. The external force acting on the rubber matrix is transferred to the rigid filler through the filler-rubber bonding points, so the strength of the vulcanizate is improved. The filler-rubber bonding points are including the filler-rubber physical bonding points connected through the noncovalent bonds and filler-rubber chemical bonding points connected through the covalent bonds. The Mullins

effect should be mainly attributed to the destruction of the filler-rubber physical bonding points and chemical bonding points and the slippage of the polymer chains on the surface of the fillers (Figure 7, row 3). Under the same filler content, the better the dispersion of the filler in the rubber matrix and the better the compatibility with the rubber matrix exhibit, the more filler-rubber interaction points are formed. The more filler-rubber interaction points are destroyed during the stretching process, the more obvious Mullins effect. This is why the Mullins effect of NR/GCB is stronger than that of NR/CB when the filler is below 20 phr.

(3) For the polymer vulcanizate system with high filler content, the more filler-rubber interaction points are formed because of the bigger filler content; thus the strength is improved. But when the addition amount of the filler is too big, the filler-filler 3D network structure will be formed in the rubber matrix, thus causing the filler agglomeration. The agglomeration of the filler in the rubber matrix causes the stress concentration, thereby resulting in a decrease in the tensile strength. This is why the tensile strength of the rubber is lowered when the amount of CB is increased from 50 phr to 60 phr. The Mullins effect at this time should be mainly ascribed to the destruction of the filler-filler 3D network structure during the stretching process (Figure 7, row 4). The Mullins effect resulted from the destruction of the filler-filler 3D network being greater than that caused by the destruction of the filler-rubber interaction. It can be seen from Figure 4.

4. Conclusions

(1) About 20% polyethylene glycol of the total mass was grafted on the surface of the carbon black, thus the dispersion of the carbon black in the rubber matrix and the compatibility with the rubber matrix were improved, thereby the comprehensive performance being increased.

(2) The degree of Mullins effect was increased with the increase of filler. However, when the filler addition was below 20 phr, the Mullins effect of NR/GCB was stronger than that of NR/CB. When the filler addition was over 30 phr, the Mullins effect of NR/CB was stronger than that of NR/GCB. The degree of Mullins effect of NR/GCB was only 47% of that of NR/CB when the filler addition was 60 phr. The Mullins effect was increased gradually during the high temperature treatment process because of the re-entanglement of the rubber molecular chains, regeneration of the filler-rubber interaction and filler-filler 3D network structure.

(3) For the virgin polymer vulcanizate system with no filler, the Mullins effect should be mainly attributed to the disentanglement of the polymer chains during the stretching process. For the polymer vulcanizate system with low filler content, the Mullins effect should be mainly ascribed to the destruction of the filler-rubber interaction during the stretching process. For the polymer vulcanizate system with high filler content, the Mullins effect at this time should be mainly resulted from the destruction of the filler-filler 3D network structure during the stretching process.

Data Availability

The data used to support the findings of this study are included within the article.

Conflicts of Interest

The authors declare that they have no conflicts of interest regarding the publication of this paper.

Acknowledgments

This work was supported by the Natural Science Foundation of Guangdong Province (2017A030310663, 2018A030307018, and 2018A0303070003), the Foundation of Guangdong Province Rubber/Plastic Materials Preparation & Processing Engineering Technology Development Centre (2015B090903083), Distinguished Young Talents in Higher Education of Guangdong (517053), Maoming Science and Technology Project (517055), and Guangdong Research Center for Unconventional Energy Engineering Technology (GF2018A005).

References

[1] X. Fan, H. Xu, Q. Zhang, D. Xiao, Y. Song, and Q. Zheng, "Insight into the weak strain overshoot of carbon black filled natural rubber," *Polymer Journal*, vol. 167, pp. 109–117, 2019.

[2] P. Yuvaraj, J. R. Rao, N. N. Fathima, N. Natchimuthu, and R. Mohan, "Complete replacement of carbon black filler in rubber sole with CaO embedded activated carbon derived from tannery solid waste," *Journal of Cleaner Production*, vol. 170, pp. 446–450, 2018.

[3] B. Sripornsawat, S. Saiwari, and C. Nakason, "Thermoplastic vulcanizates based on waste truck tire rubber and copolyester blends reinforced with carbon black," *Waste Management*, vol. 79, pp. 638–646, 2018.

[4] X. Du, Y. Zhang, X. Pan, F. Meng, J. You, and Z. Wang, "Preparation and properties of modified porous starch/carbon black/natural rubber composites," *Composites Part B: Engineering*, vol. 156, pp. 1–7, 2019.

[5] J. Chen, Y. Maekawa, M. Yoshida, and N. Tsubokawa, "Radiation grafting of polyethylene onto conductive carbon black and application as a novel gas sensor," *Polymer Journal*, vol. 34, no. 1, pp. 30–35, 2002.

[6] N. Tsubokawa, T. Satoh, M. Murota, S. Sato, and H. Shimizu, "Grafting of hyperbranched poly(amidoamine) onto carbon black surfaces using dendrimer synthesis methodology," *Polymers for Advanced Technologies*, vol. 12, no. 10, pp. 596–602, 2001.

[7] R. Richner, S. Müller, and A. Wokaun, "Grafted and crosslinked carbon black as an electrode material for double layer capacitors," *Carbon*, vol. 40, no. 3, pp. 307–314, 2002.

[8] Q. Yang, L. Wang, W. Xiang, J. Zhou, and J. Li, "Grafting polymers onto carbon black surface by trapping polymer radicals," *Polymer Journal*, vol. 48, no. 10, pp. 2866–2873, 2007.

[9] D. Julie, F. Bruno, and G. Pierre, "A review on the Mullins effect," *European Polymer Journal*, vol. 45, no. 3, pp. 601–612, 2009.

[10] H. Bouasse and Z. Carriere, "Sur les courbes de traction du caoutchouc vulcanize," *Annales de la faculte des sciences de Toulouse*, vol. 5, no. 3, pp. 257–283, 1903.

[11] L. Mullins, "Effect of stretching on the properties of rubber," *Rubber Chemistry and Technology*, vol. 21, no. 2, pp. 281–300, 1948.

[12] R. Dargazany and M. Itskov, "A network evolution model for the anisotropic Mullins effect in carbon black filled rubbers," *International Journal of Solids and Structures*, vol. 46, no. 16, pp. 2967–2977, 2009.

[13] E. B. da Rocha, F. N. Linhares, C. F. Gabriel, A. M. de Sousa, and C. R. Furtado, "Stress relaxation of nitrile rubber composites filled with a hybrid metakaolin/carbon black filler under tensile and compressive forces," *Applied Clay Science*, vol. 151, pp. 181–188, 2018.

[14] Q. Liu, K. Zhang, X. Zhang, and Z. Wang, "Strengthening effect of mullins effect of high- density polyethylene/ethylene–propylene–diene terpolymer thermoplastic vulcanizates under compression mode," *Journal of Thermoplastic Composite Materials*, vol. 31, no. 10, pp. 1310–1322, 2017.

[15] A. Ivanoska-Dacikj, G. Bogoeva-Gaceva, S. Rooj, S. Wießner, and G. Heinrich, "Fine tuning of the dynamic mechanical properties of natural rubber/carbon nanotube nanocomposites by organically modified montmorillonite: a first step in obtaining high-performance damping material suitable for seismic application," *Applied Clay Science*, vol. 118, pp. 99–106, 2015.

[16] J. Diani, M. Brieu, and P. Gilormini, "Effect of filler content and crosslink density on the mechanical properties of carbon-black filled SBRs," in *Proceedings of the 10th European Conference on Constitutive Models for Rubber, ECCMR X 2017*, pp. 3–10, Balkema, August 2017.

[17] C. Matthew and S. A. D. F. Davide, "Reversibility of the Mullins effect for extending the life of rubber components," *Plastics, Rubber and Composites*, vol. 5, pp. 24–31, 2018.

[18] R. Yang, Y. Song, and Q. Zheng, "Payne effect of silica-filled styrene-butadiene rubber," *Polymer Journal*, vol. 116, pp. 304–313, 2017.

[19] S. K. Srivastava and Y. K. Mishra, "Nanocarbon reinforced rubber nanocomposites: Detailed insights about mechanical, dynamical mechanical properties, payne, and mullin effects," *Nanomaterials*, vol. 8, no. 11, pp. 945–3021, 2018.

[20] F. Bueche, "Molecular basis for the mullins effect," *Journal of Applied Polymer Science*, vol. 4, no. 10, pp. 107–114.

[21] R. Houwink, "Slipping of molecules during the deformation of reinforced rubber," *Rubber Chemistry and Technology*, vol. 29, no. 3, pp. 888–893, 1956.

[22] M. A. Johnson and M. F. Beatty, "A constitutive equation for the Mullins effect in stress controlled uniaxial extension experiments," *Continuum Mechanics and Thermodynamics*, vol. 5, no. 4, pp. 301–318, 1993.

[23] G. Kraus, C. W. Childers, and K. W. Rollmann, "Stress softening in carbon black reinforced vulcanizates. strain rate and temperature effects," *Rubber Chemistry and Technology*, vol. 39, no. 5, pp. 1530–1543, 1966.

[24] G. R. Hamed and S. Hatfield, "On the role of bound rubber in carbon-black reinforcement," *Rubber Chemistry and Technology*, vol. 62, no. 1, pp. 143–156, 1989.

[25] T. A. Vilgis, J. Sommer, and G. Heinrich, "Swelling and fractal heterogeneities in networks," *Macromolecular Symposia*, vol. 93, no. 1, pp. 205–212, 1995.

[26] M. Cheng and W. Chen, "Experimental investigation of the stress–stretch behavior of EPDM rubber with loading rate effects," *International Journal of Solids and Structures*, vol. 40, no. 18, pp. 4749–4768, 2003.

[27] J. Fröhlich, W. Niedermeier, and H.-D. Luginsland, "The effect of filler-filler and filler-elastomer interaction on rubber reinforcement," *Composites Part A: Applied Science and Manufacturing*, vol. 36, no. 4, pp. 449–460, 2005.

[28] H. H. Hassan, E. Ateia, N. A. Darwish, S. F. Halim, and A. K. Abd El-Aziz, "Effect of filler concentration on the physico-mechanical properties of super abrasion furnace black and silica loaded styrene butadiene rubber," *Materials and Corrosion*, vol. 34, pp. 533–540, 2012.

[29] J. J. Brennan and D. H. Lambert, "Rubber—black interaction influence on cure level of vulcanizates," *Rubber Chemistry and Technology*, vol. 45, no. 1, pp. 94–105, 1972.

[30] J. Zhou, Y. Song, Q. Zheng, Q. Wu, and M. Zhang, "Percolation transition and hydrostatic piezoresistance for carbon black filled poly(methylvinylsilioxane) vulcanizates," *Carbon*, vol. 46, no. 4, pp. 679–691, 2008.

[31] G. Bohm, W. Tomaszewski, W. Cole, and T. Hogan, "Furthering the understanding of the non linear response of filler reinforced elastomers," *Polymer Journal*, vol. 51, no. 9, pp. 2057–2068, 2010.

[32] N. Kumar and V. V. Rao, "Hyperelastic Mooney-Rivlin model: determination and physical interpretation of material constants," *International Journal of Mechanical Engineering*, vol. 6, no. 1, pp. 43–46, 2016.

[33] W. Fu and L. Wang, "Research on Payne effect of natural rubber reinforced by graft-modified silica," *Journal of Applied Polymer*, vol. 133, no. 36, pp. 43891–43898, 2016.

[34] J. Chenal, C. Gauthier, L. Chazeau, L. Guy, and Y. Bomal, "Parameters governing strain induced crystallization in filled natural rubber," *Polymer Journal*, vol. 48, no. 23, pp. 6893–6901, 2007.